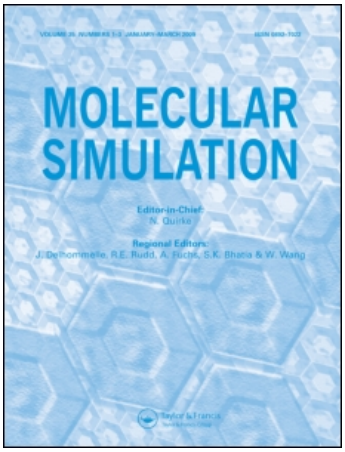

Molecular Simulation
Publication details, including instructions for authors and subscription information:
http://www.informaworld.com/smpp/title~content=t713644482

Multi-particle sampling in Monte Carlo simulations on fluids: efficiency and extended implementations

Filip Moučka[a]; Ivo Nezbeda[ab]
[a] Faculty of Science, J.E. Purkinje University, Ústí nad Labem, Czech Republic [b] E Hala Laboratory of Thermodynamics, Institute of Chemical Process Fundamentals, Academy of Sciences, Prague 6, Czech Republic

To cite this Article Moučka, Filip and Nezbeda, Ivo(2009) 'Multi-particle sampling in Monte Carlo simulations on fluids: efficiency and extended implementations', Molecular Simulation, 35: 8, 660 — 672
To link to this Article: DOI: 10.1080/08927020902725572
URL: http://dx.doi.org/10.1080/08927020902725572

Molecular Simulation
Vol. 35, No. 8, July 2009, 660–672

Taylor & Francis
Taylor & Francis Group

Multi-particle sampling in Monte Carlo simulations on fluids: efficiency and extended implementations

Filip Moučka[a] and Ivo Nezbeda[ab]*

[a]*Faculty of Science, J.E. Purkinje University, 400 96 Ústí nad Labem, Czech Republic;* [b]*E Hala Laboratory of Thermodynamics, Institute of Chemical Process Fundamentals, Academy of Sciences, 165 02 Prague 6, Czech Republic*

(*Received 5 October 2008; final version received 4 January 2009*)

Various technical aspects affecting the efficiency of a recently proposed novel Monte Carlo (MC) simulation scheme based on biased simultaneous displacements/rotations of *all* particles of the system are investigated using two polarisable models of water, the Chialvo–Cummings and Brodholt–Sampoli–Vallauri models, as a test case. Necessary expressions for polarisable site–site interaction models are derived along with a novel smoothing of the potential at the cut-off distance. In addition to the common thermodynamic and structural properties, the mean-squared displacements, rotation relaxation, speed of equilibration (translational order parameter, TOP) and autocorrelation coefficients have been computed as well, in order to assess the efficiency of the method. Gain in speed by parallelisation has also been examined. Performance of the method is coumpared with both the standard one-particle move method and the available approximate methods. It is shown that the multi-particle move (MPM) method performs about by a factor of 10 faster for the systems considered when compared with the common MC scheme, and several times faster when compared with the approximate methods. Parallelised codes of the MPM method may then perform about 70 times faster than the conventional MC. These conclusions hold true for the system size simulated ($N = 256$) because the efficiency of the multi-particle method depends on the size of the system: its efficiency even increases with increasing number of particles.

Keywords: multi-particle move; MC; parallelisation; reaction field; polarisable models of water

1. Introduction

In general, when studying molecular systems with a pairwise interaction potential by computer simulations, the choice of the method, Monte Carlo (MC) or molecular dynamics (MD), is in most cases only a matter of convenience and/or personal preference [1,2]. The preferred use of either method is dictated either by the studied system, e.g. models with a discontinuous potential favour the MC method, or the properties to be evaluated, e.g. kinetic properties are naturally obtainable from MD simulations. This sort of equivalence between the two simulation methods is however immediately lost if the pairwise additivity does not apply, an example being the polarisable models. In this case, the interaction between *all N* particles comprising the system must be evaluated in every single timestep (configuration). Since in MD simulations all particles change their positions in every timestep anyhow, this need not bring about any dramatic increase in the CPU time, but at least by a factor 2–3 in dependence on the method used to reach self-consistency of induced dipoles [3,4]. On the other hand, in common MC simulations, only the change of energy due to the change of the position or orientation of the particle attempting a move is required. Thus, for polarisable models, additional computations to determine the total interaction energy make the MC method by the factor $\mathcal{O}(N)$ slower in comparison with the MC simulations of non-polarisable models. Somewhere in between these methods, there are hybrid MD/MC methods; for a discussion of their advantages and disadvantages see, e.g. [1].

To overcome the inefficiency of MC simulations of polarisable models (and, in general, for models with non-additive interactions), we have recently proposed a novel MC method [5]. The method, called multi-particle move (MPM) MC scheme, considers simultaneous translations/rotations of all particles at once in the spirit of MD. It means that the moves are biased according to the forces acting between the molecules. To demonstrate feasibility and efficiency of the method, in [5], we considered the polarisable Stockmayer fluid. Since, however, its implementation for more complex many-site interaction models need not be straightforward, we consider in this paper the most common class of polarisable models of water and derive and present all necessary expressions. Furthermore, it turns out that the efficiency of the method is also rather sensitive to the treatment of the long-range Coulombic interactions; more accurately, to their approximation in the vicinity of the cut-off distance, and special attention has therefore been paid to this problem. A novel smoothing of the potential at the cut-off distance is

*Corresponding author. Email: ivonez@icpf.cas.cz

ISSN 0892-7022 print/ISSN 1029-0435 online

DOI: 10.1080/08927020902725572
http://www.informaworld.com

proposed and used. Finally, technical aspects affecting the efficiency of simulations, as e.g. acceptance ratio, sensitivity of the correlation length to the type of move, etc., are addressed as well along with a potential gain in speed by (simple) parallelisation. For comparison with the currently available other MC methods, we consider both the standard one-particle MC method and more efficient, but only approximate, PAPI [3,4] and ANES [6] methods. Although both latter methods have been shown to yield, if implemented with careful choice of simulation parameters, results identical to those calculated rigorously through matrix minimisation [3,4,7], both are suitable for polarisable models only and cannot be used for simulations considering other kinds of non-additive interactions.

After presenting the method in the next Section, and deriving all necessary expressions and providing all technical details for its implementation in Section 3, we then consider the Chialvo and Cummings [8] and Brodholt et al. [9] polarisable models of water and present and discuss the results in Section 4.

2. The biased MPM method

To move all particles at once in MC method without any bias would be very inefficient. The MPM method starts from the known force-bias method [10], in which the trial moves are biased in the direction of forces or torques acting on the molecules, and extends it to the simultaneous displacements (or rotations) of all particles. Thus, if F_k is the force acting on particle k to be displaced and t_m is the maximum length of any component of the translational vector, $\mathbf{t}_k$, then its components $t_k^\alpha, \alpha = 1, 2, 3$, are generated according to the probability distribution

$$\pi(t_k^\alpha) = \frac{\exp\left[\lambda\beta F_k^\alpha t_k^\alpha\right]}{\int_{-t_m}^{t_m} \exp\left[\lambda\beta F_k^\alpha t_k^\alpha\right] \mathrm{d}t_k^\alpha} = \frac{\exp\left[\lambda\beta F_k^\alpha t_k^\alpha\right]}{2\sinh\left[\lambda\beta F_k^\alpha t_m\right]/\lambda\beta F_k^\alpha}, \tag{1}$$

where $k = 1, \ldots, N$, and λ is a parameter whose value lies between 1/2 and 1 [10]; we use $\lambda = 1/2$. The acceptance probability of this move is

$$\mathrm{Prob} = \min\left\{1, \exp\left[-\beta\Delta U\right]\frac{\omega^{\mathrm{new}\to\mathrm{old}}}{\omega^{\mathrm{old}\to\mathrm{new}}}\right\}, \tag{2}$$

where

$$\omega^{\mathrm{old}\to\mathrm{new}} = \prod_{\alpha=1}^{3} \frac{\lambda\beta F_k^{\alpha,\mathrm{old}} \exp\left[\lambda\beta F_k^{\alpha,\mathrm{old}} t_k^\alpha\right]}{2\sinh\left[\lambda\beta F_k^{\alpha,\mathrm{old}} t_m\right]} \tag{3}$$

and

$$\omega^{\mathrm{new}\to\mathrm{old}} = \prod_{\alpha=1}^{3} \frac{\lambda\beta F_k^{\alpha,\mathrm{new}} \exp\left[\lambda\beta F_k^{\alpha,\mathrm{new}}(-t_k^\alpha)\right]}{2\sinh\left[\lambda\beta F_k^{\alpha,\mathrm{new}} t_m\right]}, \tag{4}$$

where ΔU is the associated change in the internal energy, and $\beta = 1/k_\mathrm{B}T$, where k_B is the Boltzmann constant and T is the absolute temperature.

The above expressions, written for the conventional one-particle translational move, are easily extended to MPMs (for details see the original paper [5]):

$$\omega^{\mathrm{old}\to\mathrm{new}} = \prod_{\alpha=1}^{3}\prod_{k=1}^{N} \omega_k^{\alpha,\mathrm{old}\to\mathrm{new}}, \tag{5}$$

where again

$$\omega_k^{\alpha,\mathrm{old}\to\mathrm{new}} = \frac{\lambda\beta F_k^{\alpha,\mathrm{old}} \exp\left[\lambda\beta F_k^{\alpha,\mathrm{old}} t_k^\alpha\right]}{2\sinh\left[\lambda\beta F_k^{\alpha,\mathrm{old}} t_m\right]}, \tag{6}$$

and

$$\omega^{\mathrm{new}\to\mathrm{old}} = \prod_{\alpha=1}^{3}\prod_{k=1}^{N} \omega_k^{\alpha,\mathrm{new}\to\mathrm{old}}. \tag{7}$$

A formula for generating the translation vector is obtained by inverting Equation (1),

$$t_k^\alpha = \frac{\ln\left[\exp\left(-\lambda\beta F_k^{\alpha,\mathrm{old}} t_m\right) + 2u_k^\alpha \sinh\left(\lambda\beta F_k^{\alpha,\mathrm{old}} t_m\right)\right]}{\lambda\beta F_k^{\alpha,\mathrm{old}}}, \tag{8}$$

where u_k^α is a random number within the interval $(0, 1)$.

A similar modification applies to the rotational move that can be implemented in a number of different ways. In this work, particle k attempts the rotation around a randomly chosen vector $\mathbf{r}_k$ whose length determines the value of the rotation angle. Thus, if $\mathbf{M}_k$ is the torque acting on particle k to be rotated and r_m is the maximum length of any component of the rotational vector $\mathbf{r}_k$, then its components are generated according to the formula

$$r_k^\alpha = \frac{\ln\left[\exp\left(-\lambda\beta M_k^{\alpha,\mathrm{old}} r_m\right) + 2u_k^\alpha \sinh\left(\lambda\beta M_k^{\alpha,\mathrm{old}} r_m\right)\right]}{\lambda\beta M_k^{\alpha,\mathrm{old}}}. \tag{9}$$

When deriving this formula, we have followed the same reasoning as in Equation (8) considering the relation $\triangle U \approx (\mathbf{M}_k \cdot \mathbf{r}_k)$ instead of $\triangle U \approx (\mathbf{F}_k \cdot \mathbf{t}_k)$. The acceptance probability is given by the same general formula as for translations, Equation (2), with F_k^α being replaced by M_k^α, t_k^α by r_k^α and t_m by r_m in Equations (3) and (4).

When generating a trial configuration, one can follow two possible scenarios: (1) let each particle to decide, with a certain probability p_r, whether to attempt rotation or translation (each-particle-decides scenario) or (2) all particles are subject to rotation at once with probability p_r, otherwise all of them are displaced (all-particles-same scenario). In both cases, each particle is translated or

rotated independently of translations and rotations of other particles by vectors $\mathbf{t}_k$ or $\mathbf{r}_k$, respectively, according to Equation (8) or (9).

3. Implementation and simulation details

Implementation of the MPM method for polarisable site–site models is considerably different from that considered in the original paper—the polarisable Stockmayer potential. To keep the considerations as general as possible but keeping simultaneously in mind the most common models of water, TIPiP models [11–13], we will consider here a general site–site potential model with one Lennard-Jones (LJ) site referred to as the oxygen (O) site, several Coulombic sites and an induced dipole moment located in the centre of mass (P). The total configurational energy is thus given by

$$U = U_{\mathrm{LJ}} + U_{\mathrm{qq}} + U_{\mathrm{pol}}, \tag{10}$$

where U_{LJ} is the energy due to the LJ interactions between the O-sites, U_{qq} stands for the charge–charge interactions and U_{pol} is the contribution due to the polarisation:

$$U_{\mathrm{LJ}} = \sum_{i<j} u_{\mathrm{LJ},ij} = 4\varepsilon \sum_{i<j} \left(\left(\frac{\sigma}{R_{i\mathrm{O},j\mathrm{O}}} \right)^{12} - \left(\frac{\sigma}{R_{i\mathrm{O},j\mathrm{O}}} \right)^{6} \right), \tag{11}$$

$$U_{\mathrm{qq}} = \sum_{i<j} u_{\mathrm{qq},ij} = \frac{1}{4\pi\varepsilon_0} \sum_{i<j} \sum_{\alpha,\beta} \frac{q_\alpha q_\beta}{R_{i\alpha,j\beta}}, \tag{12}$$

$$U_{\mathrm{pol}} = -\frac{1}{2} \sum_i (\mathbf{p}_i \cdot \mathbf{E}^q_{i\mathrm{P}}). \tag{13}$$

In the above equations $R_{i\alpha,j\beta} = |\mathbf{R}_{i\alpha,j\beta}|$ is the site–site separation between site α of molecule i and site β of molecule j, $\mathbf{p}_i$ is the induced dipole moment of molecule i, and $\mathbf{E}^q_{i\mathrm{P}}$ is the electric field at the centre of the induced dipole of molecule i originating in the Coulombic sites of the other molecules of the system,

$$\mathbf{E}^{\mathrm{q}}_{i\mathrm{P}} = \frac{1}{4\pi\varepsilon_0} \sum_{j\neq i} \sum_{\alpha} \frac{q_\alpha \mathbf{R}_{i\mathrm{P},j\alpha}}{R^3_{i\mathrm{P},j\alpha}}. \tag{14}$$

The induced dipoles are assumed to be proportional to the total electric field acting at their centres,

$$\mathbf{p}_i = \alpha(\mathbf{E}^{\mathrm{q}}_{i\mathrm{P}} + \mathbf{E}^{\mathrm{p}}_{i\mathrm{P}}), \tag{15}$$

where α is the scalar polarisability and $\mathbf{E}^{\mathrm{p}}_{i\mathrm{P}}$ is the electric field at the centre of the induced dipole of molecule i originating in the induced dipoles of the other molecules of the system,

$$\mathbf{E}^{\mathrm{p}}_{i\mathrm{P}} = \frac{1}{4\pi\varepsilon_0} \sum_{j\neq i} \left(\frac{(3\mathbf{p}_j \cdot \mathbf{R}_{i\mathrm{P},j\mathrm{P}})\mathbf{R}_{i\mathrm{P},j\mathrm{P}}}{R^5_{i\mathrm{P},j\mathrm{P}}} - \frac{\mathbf{p}_j}{R^3_{i\mathrm{P},j\mathrm{P}}} \right). \tag{16}$$

To determine the contribution of the polarisable part to the total energy, one has to evaluate first the value of the induced dipoles from Equation (15).

To handle the long-range interactions, we use the reaction field method [14]. It means that the interaction energy of particle i is given by two contributions: (1) its interaction with all particles within the sphere at the centre of mass (i.e. site P) of particle i and the cut-off radius R_c and (2) the interaction with the dielectric continuum representing the particles outside this sphere. Because of the large value of permittivity of water and the fact that the prefactor $(\varepsilon_{\mathrm{RF}} - 1)/(2\varepsilon_{\mathrm{RF}} + 1)$ tends to $1/2$ for large $\varepsilon_{\mathrm{RF}}$, we set $\varepsilon_{\mathrm{RF}} = \infty$. This formalism gives rise to additional terms and the equations must therefore be modified accordingly:

$$\begin{aligned} U_{\mathrm{LJ,cut}} &= \sum_{i<j} H(R_c - R_{i\mathrm{O},j\mathrm{O}}) u_{\mathrm{LJ},ij} + U_{\mathrm{LJcorr}} \\ &= 4\varepsilon \sum_{i<j} H(R_c - R_{i\mathrm{O},j\mathrm{O}}) \left(\left(\frac{\sigma}{R_{i\mathrm{O},j\mathrm{O}}} \right)^{12} \right. \\ &\quad \left. - \left(\frac{\sigma}{R_{i\mathrm{O},j\mathrm{O}}} \right)^{6} \right) + U_{\mathrm{LJcorr}}, \end{aligned} \tag{17}$$

$$\begin{aligned} U_{\mathrm{qq,RF}} = \frac{1}{4\pi\varepsilon_0} \sum_{i<j} H(R_c - R_{i\mathrm{P},j\mathrm{P}}) \sum_{\alpha,\beta}^{3} \frac{q_{i\alpha} q_{j\beta}}{R_{i\alpha,j\beta}} \left(1 + \frac{1}{2} \left(\frac{R_{i\alpha,j\beta}}{R_c} \right)^3 \right) \\ - \frac{N}{8\pi\varepsilon_0 R_c^3} \left(\sum_\alpha q_\alpha \mathbf{R}_{i\alpha} \right)^2, \end{aligned} \tag{18}$$

$$U_{\mathrm{pol,RF}} = -\frac{1}{2} \sum_i \mathbf{p}_{i,\mathrm{RF}} \cdot \mathbf{E}^{\mathrm{q}}_{i\mathrm{P,RF}}, \tag{19}$$

$$\begin{aligned} \mathbf{E}^{\mathrm{q}}_{i\mathrm{P,RF}} &= \frac{1}{4\pi\varepsilon_0} \sum_{j\neq i} H(R_c - R_{i\mathrm{P},j\mathrm{P}}) \\ &\quad \times \sum_\alpha \frac{q_\alpha \mathbf{R}_{i\mathrm{P},j\alpha}}{R^3_{i\mathrm{P},j\alpha}} \left(1 - \left(\frac{R_{i\mathrm{P},j\alpha}}{R_c} \right)^3 \right) \\ &\quad + \frac{1}{4\pi\varepsilon_0 R_c^3} \sum_\alpha q_\alpha \mathbf{R}_{i\alpha}, \end{aligned} \tag{20}$$

$$\mathbf{p}_{i,\mathrm{RF}} = \alpha(\mathbf{E}^{\mathrm{q}}_{i\mathrm{P,RF}} + \mathbf{E}^{\mathrm{p}}_{i\mathrm{P,RF}}), \tag{21}$$

$$\begin{aligned} \mathbf{E}^{\mathrm{p}}_{i\mathrm{P,RF}} = \frac{1}{4\pi\varepsilon_0} \sum_{j\neq i} H(R_c - R_{i\mathrm{P},j\mathrm{P}}) \left(\frac{3\mathbf{p}_{j,\mathrm{RF}} \cdot \mathbf{R}_{i\mathrm{P},j\mathrm{P}} \mathbf{R}_{i\mathrm{P},j\mathrm{P}}}{R^5_{i\mathrm{P},j\mathrm{P}}} \right. \\ \left. - \frac{\mathbf{p}_{j,\mathrm{RF}}}{R^3_{i\mathrm{P},j\mathrm{P}}} \left(1 - \left(\frac{R_{i\mathrm{P},j\mathrm{P}}}{R_c} \right)^3 \right) \right) + \frac{\mathbf{p}_{i,\mathrm{RF}}}{4\pi\varepsilon_0 R_c^3}, \end{aligned} \tag{22}$$

where H is the Heaviside step function.

The above equations constitute the standard method used in the conventional MC simulations and they can also be used in the MPM method. Their implementation in the MPM method is straightforward but rather inefficient. The problem lies in that when a particle is displaced, the number of molecules within its reaction sphere may change considerably giving rise to a large change in energy which cannot be predicted via the linearisation of the configuration energy and which is the principal of the force bias method. In other words, the configuration energy can change more or less independently of the forces acting on the particles only because of the varying number of the particles inside the reaction spheres. This fact plays a significant role, especially at higher densities and lower temperatures (ambient conditions). Consequently, one is forced to use much smaller values of the translational vector to maintain a reasonable acceptance ratio that evidently lowers the efficiency of the entire method. To demonstrate the problem with the discontinuity in the internal energy, we measured the internal energy as a function of the displacement along any randomly selected direction of a randomly selected particle. A typical result demonstrating the step behaviour of the energy is shown in Figure 1 (conventional RF curve). It is discernible that even for very small displacements, significant differences in the energies are observed. To overcome this problem, the potential must be smoothed at the cut-off distance. For simple potentials this is straightforward, whereas for the site–site models it is not so simple and various methods can be found in literature (for a discussion on the cut-off and smoothing see, e.g. [15]). For the purpose of this study, we have developed and used another method based on an averaging of $U_{ij,\mathrm{qq,RF}}$ over a certain range about the cut-off distance. The idea behind the averaging of the potential is rather simple. The cut-off radius R_c of the dielectric cavity of the conventional RF approach can be chosen arbitrarily, more or less without a significant influence on the structural properties, from the interval from about 8 Å to $L/2$ [16], where L is the simulation box size. It means, all the forms of the cut-off of the intermolecular reaction field potential with different R_c, which is taken from the appropriately chosen interval, can be considered as proper. An averaged potential, obtained by blending together these proper forms of the conventional reaction field potential should be thus proper, too. Thus, to get a smooth potential, instead of $U_{ij,\mathrm{qq,RF}}$, we have used an intermolecular potential $U_{ij,\mathrm{qq,BRF}}$ obtained by averaging $U_{ij,\mathrm{qq,RF}}$ potentials over an interval (R_{c_1}, R_{c_2}):

$$U_{ij,\mathrm{qq,BRF}} = \frac{1}{R_{c_2} - R_{c_1}} \int_{R_{c_1}}^{R_{c_2}} U_{ij,\mathrm{qq,RF}}(R_c; \ldots)\, \mathrm{d}R_c. \qquad (23)$$

In Figure 1, we show (smooth U_{qq}; conventional U_{pol} curve) that the jumps in the energy are smaller, in contrast to those of the conventional reaction field curve, but they still persist because there is another discontinuity embodied in the polarisable term of energy $U_{\mathrm{pol,RF}}$ caused by the discontinuities of $\mathbf{E}^{\mathrm{q}}_{i\mathrm{P,RF}}$ and $\mathbf{E}^{\mathrm{p}}_{i\mathrm{P,RF}}$. To remove them, the same procedure can be applied. Hence,

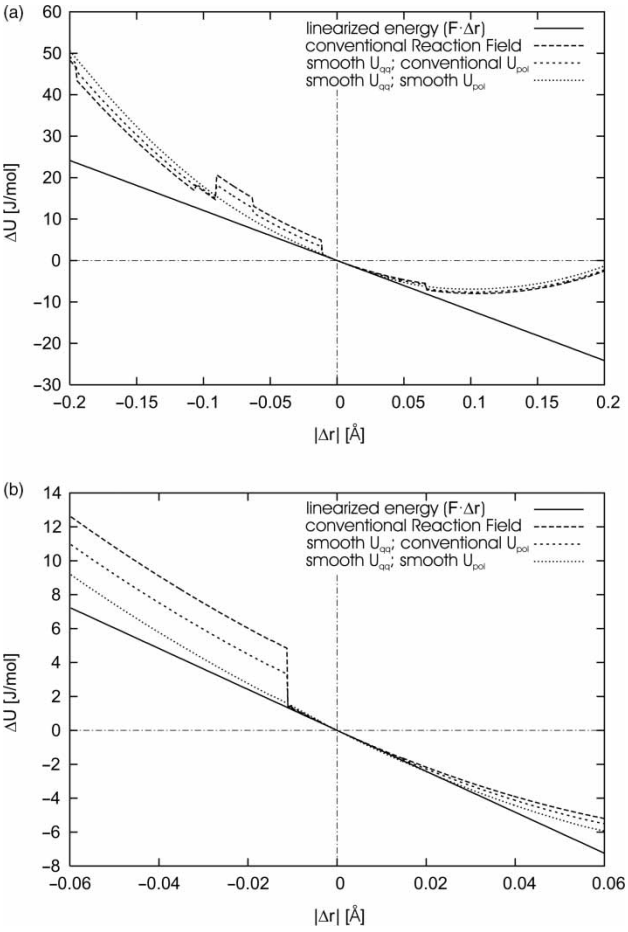

Figure 1. Typical behaviour of the internal energy during the translation of a randomly chosen molecule along any randomly selected constant direction using different reaction field smoothings and the linearised energy: large scale (top), detail (bottom).

$$\mathbf{E}^{\mathrm{q}}_{i\mathrm{P,BRF}} = \frac{1}{R_{c_2} - R_{c_1}} \int_{R_{c_1}}^{R_{c_2}} \mathbf{E}^{\mathrm{q}}_{i\mathrm{P,RF}}(R_c; \ldots)\, \mathrm{d}R_c, \qquad (24)$$

$$\mathbf{E}^{\mathrm{p}}_{i\mathrm{P,BRF}} = \frac{1}{R_{c_2} - R_{c_1}} \int_{R_{c_1}}^{R_{c_2}} \mathbf{E}^{\mathrm{p}}_{i\mathrm{P,RF}}(R_c; \ldots)\, \mathrm{d}R_c, \qquad (25)$$

$$\mathbf{p}_{i,\mathrm{BRF}} = \alpha(\mathbf{E}^{\mathrm{q}}_{i\mathrm{P,BRF}} + \mathbf{E}^{\mathrm{p}}_{i\mathrm{P,BRF}}) \qquad (26)$$

and the polarisable energy is then

$$U_{\mathrm{pol,BRF}} = -\frac{1}{2} \sum_i (\mathbf{p}_{i,\mathrm{BRF}} \cdot \mathbf{E}^{\mathrm{q}}_{i\mathrm{P,BRF}}). \qquad (27)$$

Few words on smoothing the energy (forces) at the cut-off seem now appropriate. In general, one should prove

that the polarisation energy is minimised if the smoothed functions $\mathbf{E}^{\mathrm{q}}_{i\mathrm{P,BRF}}$ and $\mathbf{E}^{\mathrm{p}}_{i\mathrm{P,BRF}}$ are used for the evaluation of Equation (27) instead of the conventional RF electrostatics. However, every method for handling the long-range electrostatic interactions is only an approximation. Moreover, the systematic error due to the smoothing is, in most cases, negligible in comparison with the statistical one. The behaviour of the internal energy in dependence on the displacement after the application of the above smoothing procedures for both U_{qq} and U_{pol} is also shown in Figure 1 (smooth U_{qq}; smooth U_{pol} curve) for comparison. As one can see, there are no energy discontinuities during the translations of the particles and the energy changes can be estimated by the products of the forces and the translational vectors ($\mathbf{F}_i \cdot \Delta\mathbf{r}_i$), much better.

Finally, to implement the MPM method, the forces and torques acting on the molecules have to be determined. In fact, it is not necessary to know their exact values because they affect only the choice of subsequent configurations (walk in the configuration space) but not the thermodynamic values at equilibrium. Performing simple algebra, one can derive the equations for the forces and torques. For the force acting on the particle i, we use

$$\mathbf{F}_i = \mathbf{F}_{i,\mathrm{LJ,cut}} + \mathbf{F}_{i,\mathrm{qq,BRF}} + \mathbf{F}_{i,\mathrm{pq,BRF}} + \mathbf{F}_{i,\mathrm{qp,BRF}} + \mathbf{F}_{i,\mathrm{pp,BRF}}, \tag{28}$$

where $\mathbf{F}_{i,\mathrm{LJ,cut}}$ is the force on the oxygen site from other oxygens, $\mathbf{F}_{i,\mathrm{qq,BRF}}$ is the force on the partial charge sites from the partial charges of the other molecules, $\mathbf{F}_{i,\mathrm{pq,BRF}}$ is the force on the induced dipole site from the partial charges of the other molecules, $\mathbf{F}_{i,\mathrm{qp,BRF}}$ is the force on the partial charge sites from the induced dipoles of the other molecules, and $\mathbf{F}_{i,\mathrm{pp,BRF}}$ is the force on the induced dipole site from the induced dipoles of the other molecules. Deriving the expressions for the forces, one has to keep in mind that the site–site interactions are not central due to the potential smoothing; the contributions to $\mathbf{F}_{i,\mathrm{pq,BRF}}$ can be calculated during the evaluation of $\mathbf{F}_{i,\mathrm{qp,BRF}}$ using Newton's third law.

Since the local fields at all particle positions are dependent on each other, an iterative technique is the common method to solve the set of Equations (15) and (16) to obtain the self-consistent contribution to the total energy. This is usually a fast-converging process with the criterion [17]

$$\max_{k=1,\ldots,N} \frac{|\mathbf{p}_k(n) - \mathbf{p}_k(n-1)|}{|\mathbf{p}_k(n)|} < 10^{-m} \tag{29}$$

used to terminate the iteration; we always used $m = 5$. The number of iteration loops was about 12 for the MPM MC and 8 for the conventional MC. It is worth recalling that Jedlovszky and Richardi [18] used much softer criterion to terminate the iteration, $m = 3$, in order to speed up the simulation, and Predota et al. [4] used some times even softer one.

In the NVT simulations, we evaluated both the common thermodynamic properties, the internal energy and the dielectric constant and the relevant structural properties, the site–site correlation functions g_{ij} and the dipole–dipole correlation functions G_l, $l = 1, 2$ [16]. The latter functions, also called 'local g factors', provide information on the mutual alignment of dipoles; moreover, they may also be used as an alternative route to the dielectric constant, see e.g. [19]. In this paper, we evaluate the static dielectric constant, ε_r, from the expression [4]:

$$\varepsilon_r = 1 + \frac{\rho\tau^2}{3\varepsilon_0 k_{\mathrm{B}} T}, \tag{30}$$

where τ^2 is the fluctuation of the total dipole moment $\mathbf{M} = \sum_{i=1}^{N}(\boldsymbol{\mu}_i + \mathbf{p}_i)$ of the simulation box per molecule,

$$\tau^2 = \frac{\langle \mathbf{M}^2 \rangle - \langle \mathbf{M} \rangle^2}{N}. \tag{31}$$

To be able to assess the efficiency of the method, in addition to the above quantities, we computed also three measures, the TOP [20], the rotational relaxation parameter of the first order (re-orientation of a molecule-fixed unit vector), RRP [21] and the mean-squared displacement, mean square displacement (MSD) [2]. The measures are defined as follows:

$$\mathrm{TOP}(t) = \frac{1}{N}\sum_{i=1}^{N} \sqrt{\langle \cos(\mathbf{k}\cdot\mathbf{r}_i(t)) \rangle^2 + \langle \sin(\mathbf{k}\cdot\mathbf{r}_i(t)) \rangle^2}, \tag{32}$$

$$\mathrm{RRP}(t) = \frac{1}{N}\sum_{i=1}^{N} \langle \boldsymbol{\nu}_i(t)\boldsymbol{\nu}_i(0) \rangle, \tag{33}$$

$$\mathrm{MSD}(t) = \frac{1}{N}\sum_{i=1}^{N} \frac{\langle |\mathbf{r}_i(t) - \mathbf{r}_i(0)|^2 \rangle}{t}, \tag{34}$$

where $\mathbf{k} = (-1, 1, -1)$, $\mathbf{r}(t)$ is the position of the particle at time (configuration) t, and averaging is performed over all particles of the sample. We remark that the used TOP given by Equation (32) differs from that given in [2]; the latter is not origin independent and may yield even unphysical results [20]. Finally, for more accurate efficiency measurements, we calculated also the auto-correlation coefficients of equilibrium thermodynamic properties according to the following formula [22]:

$$c(k) = \frac{1/(n-k)\sum_{i=1}^{n-k} \Delta X_i \Delta X_{i+k}}{(1/n)\sum_{i=1}^{n} \Delta X_i^2}, \tag{35}$$

where n is the data count and X_i is the ith measured value of the considered thermodynamic property. The faster the

autocorrelation coefficient converges to zero with increasing k, the more efficient the simulation is because the time necessary to generate two subsequent uncorrelated configurations is shorter.

The results reported in the next Section were obtained using 256 and 500 particles. Most simulations were however carried out with the former number of particles, whereas the latter one served mainly for checking purposes only. In all the simulations, we used the Lennard-Jones interaction cut-off $R_{c,\mathrm{LJ}} = 9\,\text{Å}$. In the conventional MC simulations, we used the reaction field without any smoothing and cut-off $R_c = 9\,\text{Å}$. This cut-off value was used by Predota et al. [3,4] and is therefore used also here for a fair comparison. For MPM MC, we used the same cut-offs; however, in the case of smoothing, the electrostatic contributions were smoothed over the interval $R_c \in (8.8\,\text{Å}, 9\,\text{Å})$. We found that the efficiencies of the all-particles-same and each-particle-decides concepts are similar. Thus, the all-particles-same scenario has been used in most simulations because it provides the possibility to check separately the acceptance ratios of the moves. In the case of the MPM MC in an NPT ensemble, the volume change was realised by the standard way leading to the acceptance ratio of 0.3. The MC steps consisted of a volume change with probability 0.02, or a rotation or translation of all particles with equal probability (using $p_r = 0.5,\ t_m = 0.05\,\text{Å},\ r_m = 0.12$). The thermodynamic properties were measured after every 100 steps. In the case of the MPM MC in an NVT ensemble, there were 60 attempts between two subsequent measurements (using $p_r = 0.5,\ t_m = 0.07\,\text{Å},\ r_m = 0.12$ for state point A, and $p_r = 0.5,\ t_m = 0.12\,\text{Å},\ r_m = 0.23$ for state point C; states A and C are defined in the following section). In the conventional MC, all the properties were measured after every $3N$ molecule displacement/rotation attempts with acceptance ratios about 0.3. The maximum possible length of any component of the conventional MC translation vector was 0.5 Å for state A, and 0.9 Å for state C. The particles were rotated around uniformly randomly selected axes by uniformly generated random angles not greater than 1.2 rad for state A and 1.8 rad for state C. To measure the computation speed, and hence to compare efficiency, all the computations ran on the same hardware and all simulations started from the same configuration: FCC lattice with random orientations of the molecules, $\boldsymbol{\mu}_i = \mu\boldsymbol{\nu}_i$.

4. Results and discussion

We have implemented the above-outlined MPM MC method for the Chialvo–Cummings (CC) polarisable model of water [8], which is based on the SPC/E model [23], and the Brodholt–Sampoli–Vallauri (BSV) polarisable model [9] based on the TIP4P [24], both of them with the scalar polarisability $\alpha = 1.444\,\text{Å}^3$. For further details and the parameters of the models, we refer the reader to the original papers [8,9]. We performed both NVT and NPT simulations at two thermodynamic states: at ambient conditions, $T = 298\,\text{K}$ and number density $\rho = 0.0334\,\text{Å}^{-3}$ (NVT) or pressure $p = 1$ bar (NPT), and a slightly subcritical temperature (of real water), $T = 573\,\text{K}$ and $\rho = 0.0241\,\text{Å}^{-3}$ (NVT) or $p = 100$ bar (NPT). Following Jedlovszky and Richardi [18], we will refer to these states as A and C, respectively. These states were also considered by Predota et al. [3,4] and were therefore chosen for the sake of comparison. With respect to the complexity of the problem, both physical and computational, and the novelty of cut-off smoothing, in the following we will first demonstrate the correctness of the proposed implementation of the MPM method by presenting the results for the thermodynamic and structural properties and their comparison with those reported in Refs. [3,4,18]. Then the problem of efficiency of the method and its assessment will be addressed.

4.1 Thermodynamic and structural properties

In Tables 1 and 2, we list the results for the internal energy, the average values of the total dipole moment and the induced dipole moment of the molecules, and the dielectric constant. It seems necessary first to recall that in both [4,18], the authors report error estimates only for the internal energy but not for other properties. It is also necessary to remark that the latter results seem to be the subject of rather large errors. In state A, the MPM MC results for the average values of both the permanent and total dipoles, and for the dielectric constant, agree with the literature data. As for the energy, the agreement between the results reported by Predota et al. and those by Jedlovszky and Richardi is at the edge of their combined errors. Our average value of U lies between theirs and agrees with both of them also within the combined errors. Practically, the same applies also to the energy in state C with much less differences between the average values. Predota et al. do not report any results for other quantities at this state. We agree with Jedlovszky and Richardi for the averaged dipoles and the only difference we find is for the dielectric constant. However, with respect to the usual large uncertainty of this quantity, this is not surprising (see also the discussion below).

The equilibrium number densities obtained by the NPT simulations are shown in Table 3. In state C, the results agree, more or less, with those reported in [18]. However, in state A, they differ significantly. When examining more carefully the table in [18], we find that the listed results for non-polarisable models disagree with those reported in the literature by other authors. For instance, the number density for SPC/E water in state A reported in [18] is $0.0352\,\text{Å}^{-3}$, which corresponds to $1053\,\text{kg m}^{-3}$ and is quite off the experimental value to which the potential was

Table 1. Thermodynamic properties of the CC model obtained using different simulation methods.

	U (kJ mol^{-1})	$\langle \mathbf{p} \rangle$	$\langle \mathbf{p} + \boldsymbol{\mu} \rangle$	ε_r
state point A				
MPM				
$U_{qq,BRF}$; $U_{pol,BRF}$	−40.62 ± 0.03	0.998 ± 0.001	2.81 ± 0.01	99 ± 10
$U_{qq,BRF}$; $U_{pol,RF}$	−40.61 ± 0.05	0.999 ± 0.001	2.82 ± 0.01	87 ± 15
$U_{qq,RF}$; $U_{pol,RF}$	−40.62 ± 0.05	0.997 ± 0.002	2.81 ± 0.01	86 ± 20
[4]	−40.71 ± 0.06	1.00	2.82	90
[17]	−40.31 ± 0.35	0.978	2.792	104.8
state point C				
MPM				
$U_{qq,BRF}$; $U_{pol,BRF}$	−23.48 ± 0.02	0.582 ± 0.001	2.374 ± 0.001	21.5 ± 0.3
$U_{qq,BRF}$; $U_{pol,RF}$	−23.48 ± 0.02	0.582 ± 0.001	2.374 ± 0.001	21.7 ± 0.5
$U_{qq,RF}$; $U_{pol,RF}$	−23.51 ± 0.02	0.583 ± 0.001	2.376 ± 0.001	21.8 ± 0.5
[4]	−23.53 ± 0.02	–	–	–
[17]	−23.48 ± 0.58	0.585	2.378	17.4

Table 2. Thermodynamic properties of the BSV model (MPM MC with $U_{qq,BRF}$; $U_{pol,BRF}$).

	U (kJ mol^{-1})	$\langle \mathbf{p} \rangle$	$\langle \mathbf{p} + \boldsymbol{\mu} \rangle$	ε_r
state point A				
MPM	−41.93 ± 0.02	0.988 ± 0.001	2.808 ± 0.001	150 ± 15
[18]	−41.70 ± 0.41	0.966	2.778	132.2
state point C				
MPM	−24.305 ± 0.008	0.580 ± 0.001	2.376 ± 0.001	23.5 ± 0.3
[18]	−24.20 ± 0.55	0.576	2.365	18.4

fitted. On the other hand, the value we get using the MPM MC method is 0.033431 Å^{-3} (i.e. 1000.08 kg m^{-3}) which is much closer to the experimental measurements and agrees also with other simulation data, see e.g. [25,26]. We therefore tend to question the reliability of the data given in [18].

The site–site correlation functions are shown in Figures 2 and 3, where they are compared with those obtained by Predota et al. This comparison confirms again that the structure generated by the conventional and MPM MC methods is identical. In addition, to the site–site correlation functions $g_{\alpha\beta}$, we also computed the first two dipole–dipole correlation functions G_l; they are shown in Figure 4. These functions are not available for the studied model in literature but were reported in [19] for its parent model TIP4P, and in [27] for other polar fluids. For non-polarisable models, function G_1 is characterised by a fast decay after the first coordination shell with a small but persistent negative value over a large range of separations. It means that after the first coordination shell a certain uniform alignment can be observed [19]. For the polarisable model, G_1 also decays fast to unity after the first peak but then it exhibits an oscillatory behaviour characteristic for cut-off models.

4.2 Efficiency of the method

As mentioned above, all simulations started from the same crystalline phase. To assess the efficiency of different methods, we focussed on the rate with which the systems went over from the crystalline phase to an equilibrated disordered phase. The results are shown in Figure 5 for the TOP and RRP. As we can see, in the MPM MC method the system melts very fast (note the different time scales),

Table 3. Number densities obtained by NPT simulations for the CC and BSV models (MPM MC with $U_{qq,BRF}$; $U_{pol,BRF}$).

	state point A		state point C	
	CC	BSV	CC	BSV
ρ (10^{-2} Å^{-3})				
MPM	2.863 ± 0.001	3.377 ± 0.003	0.1485 ± 0.0002	0.1569 ± 0.0004
[18]	2.956 ± 0.046	3.622 ± 0.045	0.140 ± 0.005	0.152 ± 0.007

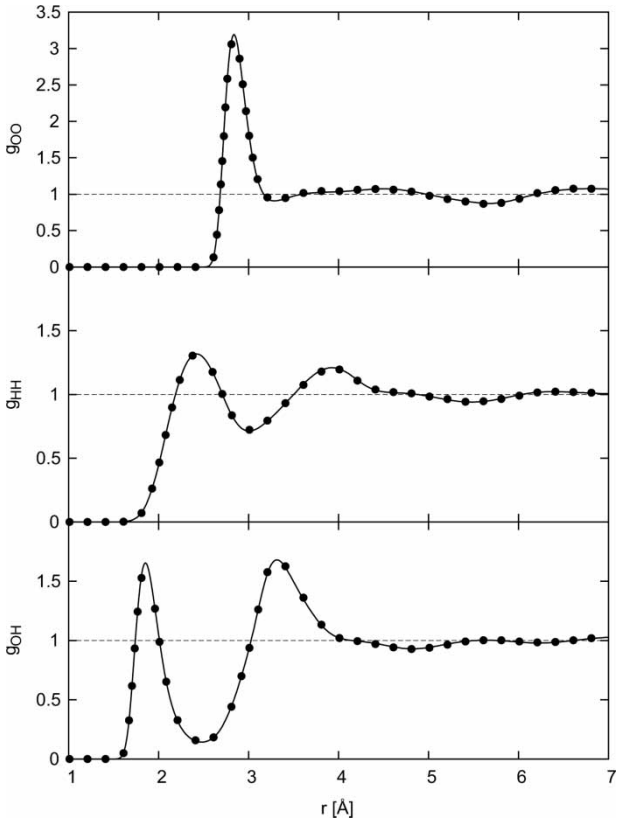

Figure 2. Comparison of the site–site correlation functions of the CC model in state A: MPM MC method with the smoothed U_{qq} and U_{pol} (this work; solid line) and the common MC method ([4]; circles).

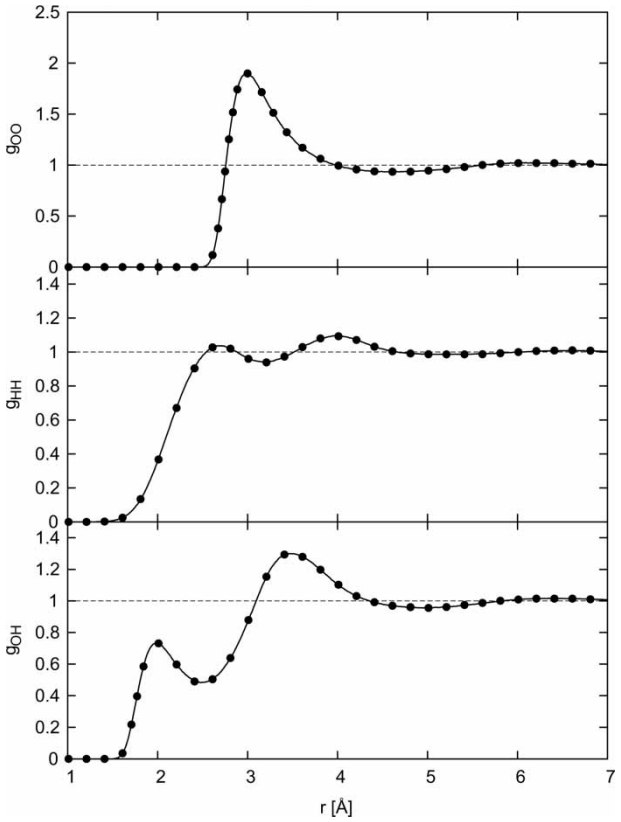

Figure 3. The same as in Figure 2 for state C.

whereas using the conventional MC it takes about by one order more time. It may be also of interest to remark that, in contrast to our previous work on the Stockmayer fluid [5], the RRP converges more slowly than the TOP because of the highly directional intermolecular potential. In Figure 6, we show the development of the total internal energy. Its rate of convergence coincides with that of TOP, suggesting the computational convenience of the biased MPM MC method and verifies that all the simulated systems reached equilibria.

A closely related question is how fast the system loses its memory. Thus, in order to eliminate the possibility of spurious fast convergence, we have followed the previous paper [5] and applied the blocking method of Flyvbjerg and Petersen ([28]) to the total energy. In Figure 7, we present an example of the resulting graphs that were analysed in order to determine the correlation lengths and associated computational times. In addition, we present a comparison of the autocorrelation coefficients of the configurational energy in Figure 8. We find that the computational correlation times, i.e. the machine time necessary to generate an independent block of configurations, are about 10 times shorter for the MPM method in comparison with the conventional single-particle MC. However, it is also fair to say that these estimates are rather approximate due to the requirement of having extremely large amount of data for the analysis and the presence of long-range correlations embodied in the polarisable models itself.

The last quantity of interest is the MSD shown in Figure 9. This quantity is related to diffusivity and reflects mobility of the molecules. As it is seen, in the biased MPM MC method, particles move much faster and thus, again, sample the configuration space much more efficiently.

We did not carry out any efficiency measurements in the NPT simulations because the only difference between the NPT and NVT simulations is an additional volume change step, which is naturally all-particle based and is thus not affected by the MPM MC.

In addition to the efficiency discussed above in terms of various measures, a direct comparison of the CPU time required by different methods would be also quite useful information. However, such a comparison can hardly be made in a fair way and only approximate or indirect estimates can be given. The approximate PAPI method, designed to perform efficiently, is governed by a number of parameters. It was reported in [4] that the combination, which is accurate and simultaneously also efficient,

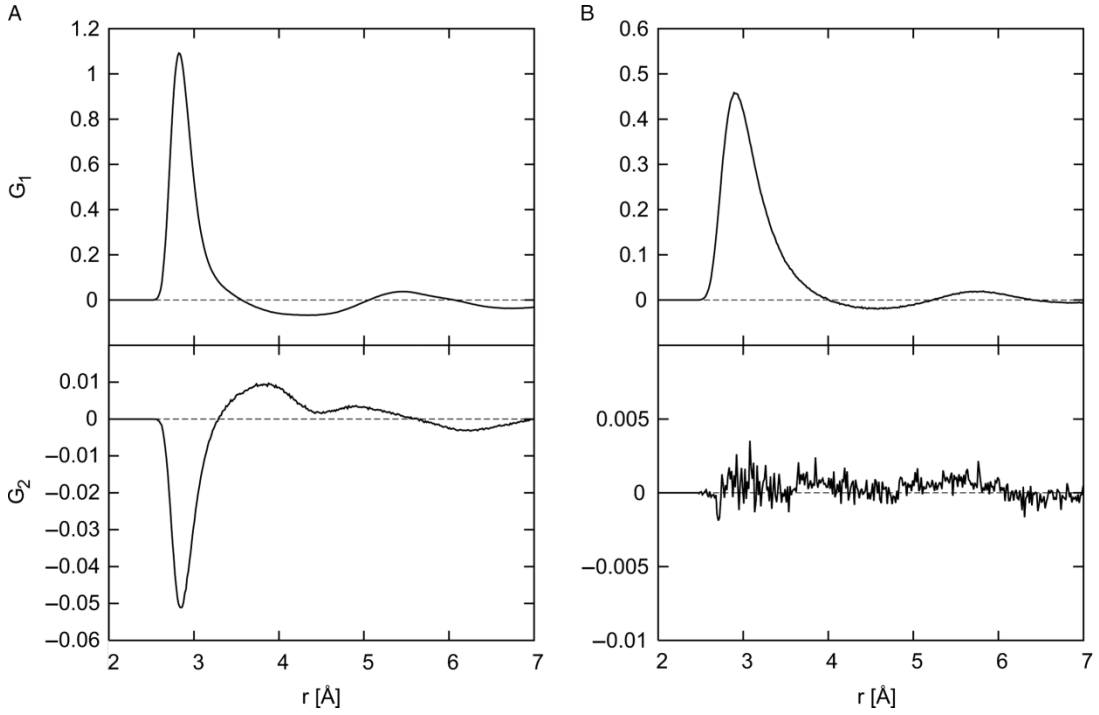

Figure 4. The dipole–dipole correlation functions of the CC model in state A (left column) and state B (right column).

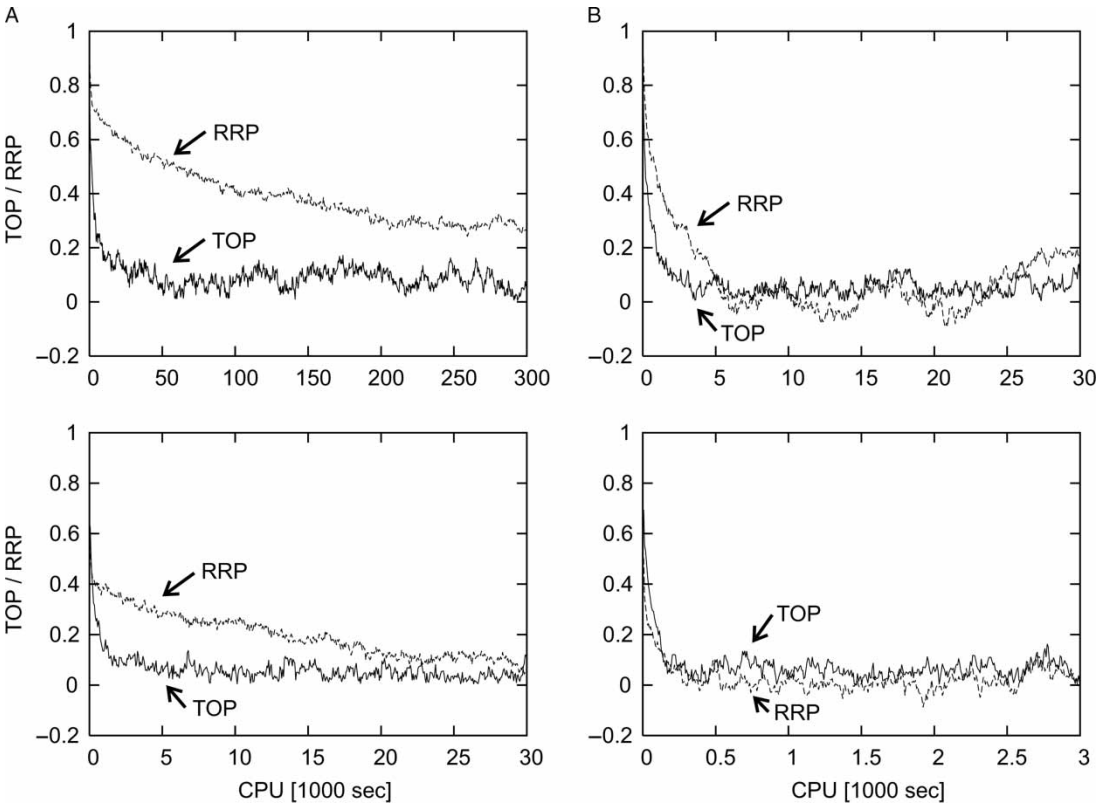

Figure 5. Comparison of the development of the TOPs and the rotational relaxation parameters (RRP) in the CC model in an NVT simulation and state A (left column) and state B (right column): the conventional MC (upper row) and the MPM MC with the smoothed U_{qq} and U_{pol} (lower row).

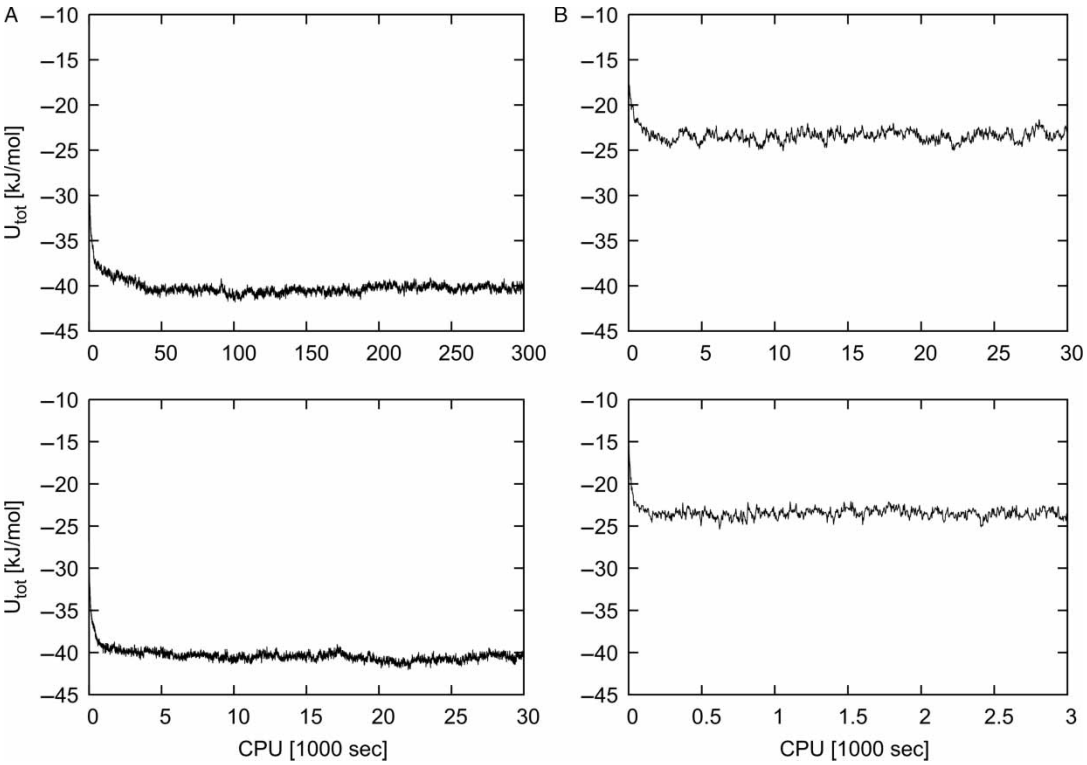

Figure 6. The same as in Figure 5 for the internal energy.

performs about five times faster in comparison with the common (exact) method. In the case of the MPM MC method, the gain in speed is one order which means that it may require only one-half of the CPU time required by (only approximate!) PAPI method. As regards the ANES method, we are not aware of any representative comparison with the conventional MC; however, computing-time requirements of this method increase only as N^2 under certain conditions (e.g. small nuclear displacements and preferential sampling) [6].

4.3 Parameter dependence

There are several simulation parameters that must be set to run the simulation and that also affect its efficiency. Dependence of the efficiency of the MPM MC on these parameters was investigated in an NVT ensemble using the polarisable BSV model at ambient conditions with 256 particles. To assess the parameter dependence, we focused on the autocorrelation coefficients of the configurational energy, U, its individual contributions (U_{LJ}, U_{qq} and U_{pol}) and the mean value of the induced dipole moment μ. Both

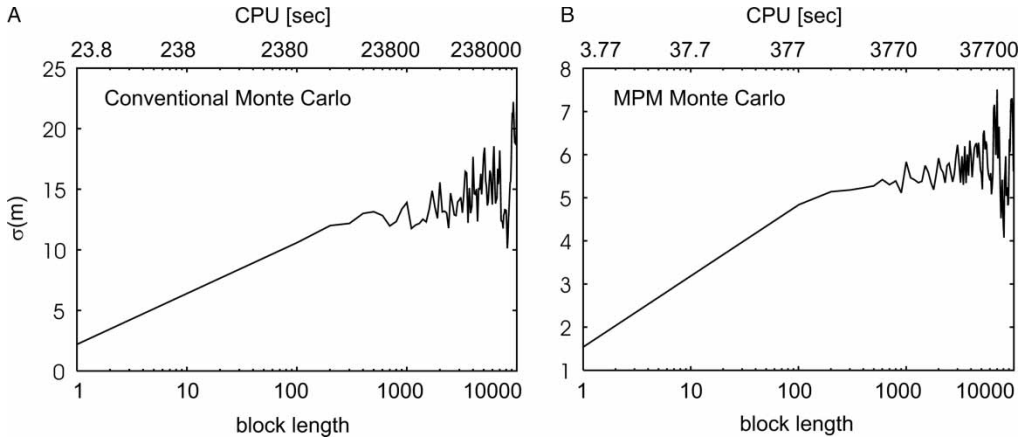

Figure 7. Block analysis of the total internal energy for state C using the CC model in the NVT ensemble: conventional MC method (left), MPM MC method with the smoothed U_{qq} and U_{pol} (right). $\sigma(m)$ is the SD.

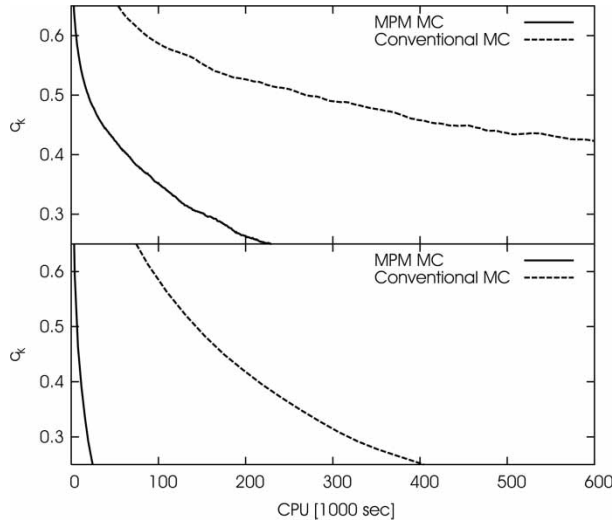

Figure 8. Autocorrelation coefficients of the total internal energy using the CC model and different methods in the NVT simulation: state A (top), state C (bottom). MPM MC is with the smoothed U_{qq} and U_{pol}.

U_{qq} and U_{pol} were smoothed as described above. In order to make the measurement of acceptance ratio of translations a_t and rotations a_r possible, trial configurations were generated using the all-particles-same scenario. It was practically impossible to examine the multiplicity of the combinations of parameters t_m, r_m and p_r. Thus, a simple iterative procedure was applied. At first, we made simulations with $r_m = 0.12$ (corresponding to the acceptance ratio of rotations of all the particles $a_r = 0.35$), $p_r = 0.5$ and $t_m = \{0.03, 0.04, 0.05, 0.06, 0.07, 0.08, 0.09, 0.1\}$ Å. The resulting autocorrelation coefficients revealed that the most convenient choice for t_m lies between 0.05 Å and 0.07 Å, whereas the corresponding acceptance ratios a_t are between 0.3 and 0.55. The efficiency of the MPM MC simulations is almost constant in this interval. Then we carried out simulations with parameters $t_m = 0.05$ Å, $p_r = 0.5$ and $r_m = \{0.04,0.06,0.08,0.09,0.10,0.11,0.13,0.14, 0.15,0.17\}$. The fastest drop of the autocorrelation coefficients was observed for r_m between 0.09 and 0.13 corresponding to a_r between 0.28 and 0.58. The efficiency dependence on p_r was explored by simulations with $t_m = 0.05$ Å, $r_m = 0.12$ and $p_r = \{0.1,0.2,0.25,0.3,0.35, 0.45,0.55,0.6,0.65,0.75,0.9\}$. The most convenient values of p_r seem to be between 0.4 and 0.6. This analysis shows that all the parameters chosen (intuitively) at the beginning of the whole procedure fall to the intervals of the most convenient values. In Figure 10, we show selected convergence profiles of the autocorrelation coefficients of the configurational energy resulting from these MPM MC simulations using different combinations of parameters.

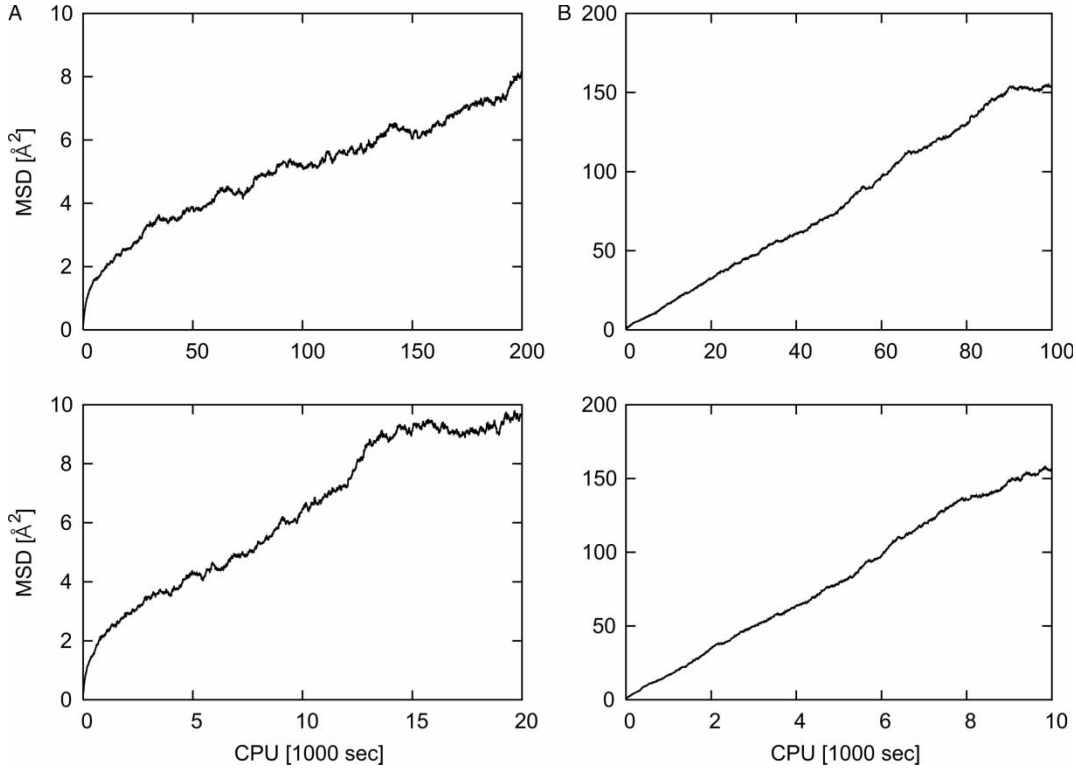

Figure 9. The same as in Figure 5 for the MSD.

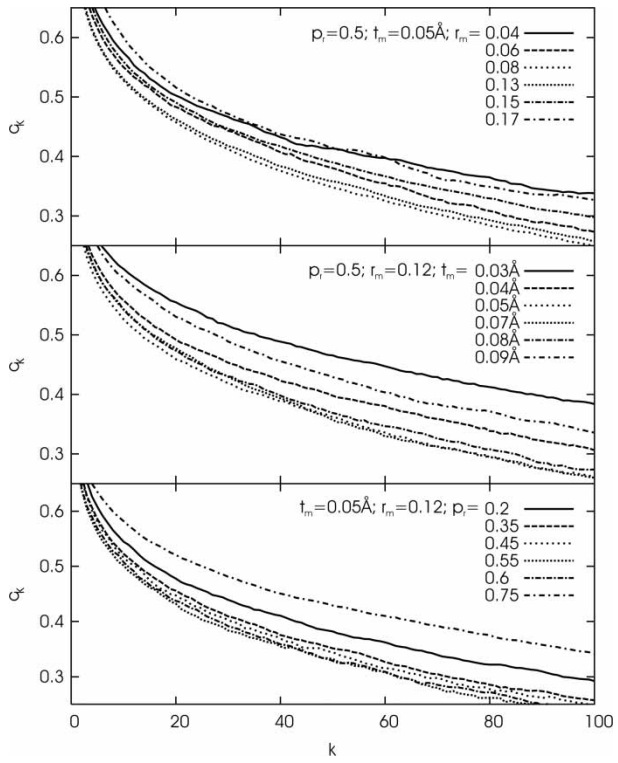

Figure 10. Comparison of the autocorrelation coefficients of U for the BSV model in state A and NVT simulations using the MPM MC with the smoothed U_{qq} and U_{pol} and different parameters.

In Table 4, we give the parameters used for the translational and rotational moves for different smoothing techniques leading to the acceptance ratios about 0.3. As it is seen, the smoothing does play the significant role for the translations in the most interesting low temperature state A. Increase in temperature diminishes differences in the energy change as it is demonstrated by the parameters for state C. Rotation does not lead to any change in the number of particles within the cut-off sphere and does not affect thus the energy change to such an extent regardless of the thermodynamic state.

Table 4. Parameters of the MPM MC moves adjusted so as to maintain the acceptance ratio about 0.3 using different smoothing methods and the CC model of water in an NVT ensemble.

	t_m (Å)	r_m (rad)
state point A: MPM		
$U_{qq,BRF}$; $U_{pol,BRF}$	0.07	0.13
$U_{qq,BRF}$; $U_{pol,RF}$	0.05	0.13
$U_{qq,RF}$; $U_{pol,RF}$	0.03	0.13
state point C: MPM		
$U_{qq,BRF}$; $U_{pol,BRF}$	0.12	0.23
$U_{qq,BRF}$; $U_{pol,RF}$	0.12	0.23
$U_{qq,RF}$; $U_{pol,RF}$	0.12	0.23

4.4 Parallelisation

The MPM MC scheme is a natural candidate of parallelisation, i.e. another possibility to speed up the computations. To this end, the MPM MC program code was parallelised and simulations of BSV polarisable model of water at ambient conditions were performed. The OpenMP directives and Intel Fortran Compiler 10.1. were used for this purpose. The computer hardware available was 14 nodes SGI AltixXE 310 (7 pieces of 1U server AltixXE 310, each containing 2 nodes) with 28 processors Intel Xeon Quad-core 5365 (frequency 300 GHz) and 16 GB shared memory DDR2 (667 MHz) at each node. Our goal was to parallelise the code for one computer node, i.e. eight computational cores with shared memory. With respect to the program structures already contained in the MPM MC, there was no problem to add a few OpenMP directives and distribute the calculation job to the individual cores efficiently. The calculations of distances and vectors between the interaction sites of molecules, calculations of non-polarisable energies and forces, iteration of induced dipoles, calculation of forces resulting from the polarisability of molecules and the initialisations of long memory fields were parallelised in this way. On the other hand, neither the computations of the MSD, TOP, RRP, and the subroutine generating trial configurations, nor the pseudo-random number generator were parallelised.

To compare the speed of computations, the program speed running on 8 cpu cores was about seven times higher than that on a single cpu (for both $N = 256$ and 500). Thus, combining the MPM MC scheme with parallelisation using a common eight-core computational node, the factor of the gain in speed has been about 70 in comparison with a common one-particle MC. Finally, to avoid any confusion, we must mention in passing that all the results concerning the efficiency and discussed in the preceding subsections were obtained without any parallelisation.

5. Conclusions

We have recently proposed a novel MC method, the MPM MC scheme, in which the trial moves of all particles are attempted simultaneously. The main gain in efficiency is due to biasing the moves with respect to the forces acting between the molecules. There is no question concerning validation of the method but its implementation need not be straightforward for complex systems. In this paper, we have considered a site–site interaction model with the Coulombic interactions and an isotropic polarisability exemplified by the CC and BSV models of water. When implementing the MPM MC method for such systems, one may also encounter problems with cut-off corrections that affect the efficiency. Whereas in the case of the common one-particle MC method even no smoothing need to be applied, in the case of the MPM MC, this becomes necessary to make the simulation really efficient (i.e. to

change the configurations from one another significantly). We have therefore introduced and tested in this paper a novel method, a sort of an average correction; but in fact, this is only a matter of a personal taste and other routines may be applied as well. If the more time-consuming Ewald summation is employed, the convenience of the MPM MC should be similar or better because using the MPM MC means greater configurational change for the same number of calculations of the configurational energy.

In contrast to the well-known Hybrid MC/MD method, the MPM MC does not require any time-consuming fine-tuning for a number of parameters and the implementation of the MPM MC is rather simple. Originally, the three parameters governing the efficiency, t_m, r_m and p_r, were set by intuition following the recommendations for the common MC simulations. It has been however shown that the range of optimal values of these parameters is rather broad and that the use of intuition is sufficient. Moreover, the MPM MC may be naturally parallelised, which is not the case of the common one-particle MC scheme. In spite of using just the simplest OpenMP directives and parallelising the most important program sections only, we obtained a very efficient tool for studying systems not only with polarisable models but, in general, with non-additive forces which is a path that will be likely followed in future development of the liquid state theory.

As for an application of the MPM MC to molecular systems with pairwise additive interactions, we have found out from our Lennard-Jones fluid simulations that the MPM MC is about seven times less efficient than the conventional MC. It is not surprising because the MPM MC has not been devised for simple systems and does not utilise additivity of the configurational energy at all. That is the reason why we decided not to present such results regarding these simple models. On the other hand, we think that the MPM MC could be an ideal candidate for nowadays massively parallel graphics processing unit computing, which is the case where the ability of efficient parallelisation can potentially overcome other aspects of the algorithm.

Acknowledgements

This work was supported by the Grand Agency of the Academy of Sciences of the Czech Republic (grant no. IAA400720802). Valuable discussions with Dr M. Predota, University of South Bohemia, are also greatly acknowledged.

References

[1] D. Frenkel and B. Smit, *Understanding Molecular Simulation*, Academic Press, San Diego, CA, 2002.

[2] M.P. Allen and D.J. Tildesley, *The Computer Simulation of Liquids*, Clarendon Press, Oxford, UK, 1987.

[3] M. Předota, P.T. Cummings, and A.A. Chialvo, *Pair approximation for polarization interaction: efficient method for Monte Carlo simulations of polarizable fluids*, Mol. Phys. 99 (2001), pp. 349–354.

[4] M. Předota, P.T. Cummings, and A.A. Chialvo, *Pair approximation for polarization interaction and adiabatic nuclear and electronic sampling method for fluids with dipole polarizability*, Mol. Phys. 100 (2002), pp. 2703–2717.

[5] F. Moučka, M. Rouha, and I. Nezbeda, *Efficient multiparticle sampling in Monte Carlo simulations on fluids: application to polarizable models*, J. Chem. Phys. 126 (2007), pp. 224106–224108.

[6] B. Chen and J.I. Siepmann, *Monte Carlo algorithms for simulating systems with adiabatic separation of electronic and nuclear degrees of freedom*, Theor. Chem. Acc. 103 (1999), pp. 87–104.

[7] B. Chen, J.J. Potoff, and J.I. Siepmann, *Adiabatic nuclear and electronic sampling Monte Carlo simulations in the Gibbs ensemble: application to polarizable force fields for water*, J. Phys. Chem. B 104 (2000), pp. 2378–2390.

[8] A.A. Chialvo and P.T. Cummings, *Engineering a simple polarizable model for the molecular simulation of water applicable over wide ranges of state conditions*, J. Chem. Phys. 105 (1996), pp. 8274–8281.

[9] J. Brodholt, M. Sampoli, and R. Vallauri, *Parameterizing a polarizable intermolecular potentials for water*, Mol. Phys. 86 (1995), pp. 149–158.

[10] C. Pangali, M. Rao, and B.J. Berne, *On a novel Monte Carlo Scheme for simulating water and aqueous solutions*, Chem. Phys. Lett. 55 (1978), pp. 413–417.

[11] B. Guillot, *A reappraisal of what we have learnt during three decades of computer simulations on water*, J. Mol. Liq. 101 (2002), pp. 219–260.

[12] S.W. Rick, *A reoptimization of the five-site water potential (TIP5P) for use with Ewald sums*, J. Chem. Phys. 120 (2004), pp. 6085–6093.

[13] J.L.F. Abascal and C. Vega, *A general purpose model for the condensed phases of water: TIP4P/2005*, J. Chem. Phys. 123 (2005), pp. 234505–234512.

[14] M. Neumann and O. Steinhauser. *The influence of boundary conditions used in machine simulations on the structure of polar systems*, Mol. Phys. 39 (1980), pp. 437–454.

[15] I.P. Omelyan, *On the reaction field for interation site models of polar systems*, Phys. Lett. A 223 (1996), pp. 295–302.

[16] O. Steinhauser, *Reaction field simulation of water*, Mol. Phys. 45 (1982), pp. 335–348.

[17] F.J. Vesely, *N-particle dynamics of polarizable Stockmayer-type molcules*, J. Comput. Phys. 24 (1977), pp. 361–371.

[18] P. Jedlovszky and J. Richardi, *Comparison of different water models from ambient to supercritical conditions: a Monte Carlo simulation and molecular Ornstein-Zernike study*, J. Chem. Phys. 110 (1999), pp. 8019–8031.

[19] J. Kolafa and I. Nezbeda, *Effect of short- and long-range forces on the structure of water. II. Orientational ordering and the dielectric constant*, Mol. Phys. 98 (2000), pp. 1505–1520.

[20] Computational Chemistry List, *Fiche F. 25. Routine to calculate translational order parameter*. Available at: http://www.ccl.net/cca/software/SOURCES/FORTRAN/allen-tildesley-book/f.25.shtml

[21] R. Witt, L. Sturz, A. Doelle, and F. Mueller-Plathe, *Molecular dynamics of benzene in neat liquid and a solution containing polystyrene. 13C nuclear magnetic relaxation and molecular dynamics simulation results*, J. Phys. Chem. A 104 (2000), pp. 5716–5725.

[22] J. Kolafa and J.W. Perram, *Cutoff errors in the Ewald summation formulae for point charge systems*, Mol. Simul. 9 (1992), pp. 351–368.

[23] H.J.C. Berendsen, J.R. Griega, and T.P. Straatsma, *The missing term in effective pair potentials*, J. Phys. Chem. 91 (1987), pp. 6269–6271.

[24] W.L. Jorgensen, J. Chandrasekhar, J.D. Madura, R.W. Impey, and M.L. Klein, *Comparison of simple potential functions for simulating liquid water*, J. Chem. Phys. 79 (1983), pp. 926–935.

[25] W.L. Jorgensen and C. Jenson, *Temparature dependence of TIP3P, SPC, and TIP4P water from NPT Monte Carlo simulations: seeking a temperature of maximum density*, J. Comput. Chem. 19 (1998), pp. 1179–1186.

[26] E. Sanz, C. Vega, J.L.F. Abascal, and L.G. MacDowell, *Phase diagram of water from computer simulation*, Phys. Rev. Lett. 92 (2004), pp. 255701–255704.

[27] J. Kolafa, I. Nezbeda, and M. Lisal, *Effect of short- and long-range forces on the properties of fluids. III. Dipolar and quadrupolar fluids*, Mol. Phys. 99 (2001), pp. 1751–1764.

[28] H. Flyvbjerg and H.G. Petersen, *Error estimates on averages of correlated data*, J. Chem. Phys. 91 (1989), pp. 461–466.